Structure and composition of the ZnSe(001) surface during atomic-layer epitaxy

Akihiro Ohtake
Joint Research Center for Atom Technology (JRCAT), Tsukuba 305-0046, Japan
and Angstrom Technology Partnership (ATP), Tsukuba 305-0046, Japan

Takashi Hanada
Joint Research Center for Atom Technology (JRCAT), Tsukuba 305-0046, Japan;
National Institute for Advanced Interdisciplinary Research (NAIR), Tsukuba 305-8562, Japan;
and Institute for Materials Research, Tohoku University, Sendai 980-8577, Japan

Tetsuji Yasuda
Joint Research Center for Atom Technology (JRCAT), Tsukuba 305-0046, Japan
and National Institute for Advanced Interdisciplinary Research (NAIR), Tsukuba 305-8562, Japan

Kenta Arai and Takafumi Yao
Joint Research Center for Atom Technology (JRCAT), Tsukuba 305-0046, Japan;
National Institute for Advanced Interdisciplinary Research (NAIR), Tsukuba 305-8562, Japan;
and Institute for Materials Research, Tohoku University, Sendai 980-8577, Japan
(Received 12 November 1998; revised manuscript received 15 June 1999)

Atomic-layer epitaxy (ALE) processes of ZnSe on GaAs(001) have been studied using reflection high-energy electron diffraction (RHEED), total reflection-angle x-ray spectroscopy, and x-ray photoelectron spectroscopy. We have obtained direct evidence that the growing surface of ZnSe(001) changes its chemical composition during ALE growth, which corresponds to the alternate formation of the Se-stabilized (2×1) and Zn-stabilized $c(2\times2)$ reconstructions. The rocking-curve analysis of RHEED have been used in structure analysis for these reconstructed surfaces: the (2×1) surface has the Se-dimer structure, in agreement with previous studies. On the other hand, we have found that the $c(2\times2)$ surface has the Se-vacancy structure, contrary to the previously proposed Zn-vacancy structure. The growth rate of ZnSe has been estimated to be about 0.5 bilayer per ALE cycle, which is consistent with the formation of these surface structures. [S0163-1829(99)13235-1]

I. INTRODUCTION

Molecular-beam epitaxy (MBE) has evolved into the most refined technique for growing thin films. Atomic-layer epitaxy (ALE) is a modification of MBE, where constituent elements are alternately deposited onto substrate surfaces. Thus, ALE growth is expected to proceed stepwise, which will be of great advantage in fabricating a well-controlled heterostructure at an atomic scale.

In this paper, we report the real-time observation of ALE growth processes of ZnSe on GaAs(001). Yao and Takeda first studied ALE growth of ZnSe(001) and found that the surface reconstruction changes from (2×1) to $c(2\times2)$ by switching a Se exposure to a Zn exposure and vice versa.[1] Although a possible mechanism has been proposed for the ALE growth of ZnSe,[2] there is even no consensus as to the growth rate per one cycle of alternating beam exposure of Zn and Se: growth of 1 bilayer (BL) (Ref. 3) per cycle has been observed at 280 °C (Ref. 1) and in the range of 250 to 350 °C,[4] while Bauer *et al.*[5] and Gains and Ponzoni[6] have obtained growth rates of 0.6 BL/cycle at 250 °C and 0.5 BL/cycle at 240 °C respectively. In order to obtain details on the ALE growth mechanism, information about the atomic structure and chemical composition of the (2×1) and $c(2\times2)$ reconstructed surfaces is indispensable.

The standard technique for monitoring ALE processes is reflection high-energy electron diffraction (RHEED). On the other hand, information about chemical composition of growing surfaces, which complements the structural information available from RHEED, has so far been lacking. In order to study *both* the structure and composition of ZnSe(001) surfaces during ALE growth, we have used total reflection-angle x-ray spectroscopy (TRAXS) and RHEED. TRAXS is a method for detecting characteristic x-rays emitted from a solid surface excited by a RHEED beam.[7] We have applied this technique to evaluate the growth rate and surface-chemical composition of ZnSe(001). Atomic structures of the ZnSe(001) surface have been determined using rocking-curve analysis of RHEED. Because of the grazing-angle geometry of the electron gun and the x-ray detector, the combination of RHEED and TRAXS enables the simultaneous monitoring of the structure and composition of growing surfaces *during* deposition.

II. EXPERIMENT

The experiments were performed in a dual-chamber MBE system equipped with the RHEED, TRAXS, x-ray photoelectron spectroscopy (XPS), reflectance difference spectroscopy (RDS), and scanning tunneling microscopy appara-

tuses. After growth of an undoped homoepitaxial layer (~0.5 μm) on a thermally cleaned GaAs(001) substrate (semi-insulating and nominally on axis), the surface showed an As-stabilized (2×4) reconstruction ($\beta2$ phase), as confirmed by RHEED observations and RDS measurements.[8] The sample was then transferred via ultrahigh vacuum transfer modules to another MBE chamber for ALE growth of ZnSe. Prior to the growth, the sample was exposed to a Zn beam for 150 s at 250 °C. This treatment is known to be the optimal method to suppress the defect generation and to promote layer-by-layer growth in ZnSe heteroepitaxy on GaAs.[9,10] ALE growth of ZnSe was performed at 250 °C by alternately supplying Zn and Se for 150 s each, with a short interval of growth interruption (30 s) in between. The beam-equivalent pressures of Zn and Se were both 1.0×10^{-7} Torr. The exposure time of 150 s was long enough to obtain the transition between the Se-stabilized (2×1) and Zn-stabilized $c(2\times2)$ surfaces and to measure TRAXS spectra during the exposure.

For TRAXS measurements, the azimuthal angle between the direction of the incident electron beam and that of the emitted x-rays detected by a Si(Li) detector was fixed at 90°. The x-rays excited by the incident electron beam with an acceleration energy of 15 keV were detected at a fixed take-off angle (θ_t) of 0.2°, which is close to the critical angle for total reflection of the Se $K\alpha$ line by ZnSe. Once θ_t is set, it should be fixed during the measurements, because the x-ray intensities drastically change with a small change of θ_t (see Fig. 2 below). The azimuth and the glancing angle of the incident electron beam are [110] and 2.0°, respectively. RHEED rocking curves of the ZnSe(001) surfaces under the Se or Zn beam were measured along the [110] direction with an electron energy of 15 keV. The RHEED patterns in this direction show spots lying on a semicircle, the zeroth-order Laue zone. This is what would be expected for a well-ordered surface. On the other hand, the RHEED patterns observed along the $[1\bar{1}0]$ direction consist of streaks. Thus, only the data in the [110] direction were used in the present analysis. Intensities of the 7 spots, (0 0), ($\pm\frac{1}{2}$ 0), (±1 0), and (±2 0) for the (2×1) surface, and 5 spots, (0 0), (±1 0), and (±2 0) for the $c(2\times2)$ surface, were measured by a charge-coupled-device camera with a microcomputer system. Averaging of the intensities of symmetry-equivalent spots led to five and three independent rocking curves from the (2×1) and $c(2\times2)$ surfaces, respectively. The glancing angle of the incident electron beam was changed by using the extended beam rocking facility (Staib, EK-35-R and k-Space, kSA400) with intervals of ~0.03°.

III. RESULTS AND DISCUSSION

A. Growth mode and growth rate of ZnSe(001)

Figure 1(a) shows intensities of Zn $K\alpha$ (8.63 keV) and Se $K\alpha$ (11.21 keV) lines plotted as a function of the cycle of the number of the ALE cycles When the GaAs(001) surface was exposed to the first Zn beam, the Zn $K\alpha$ line became visible on the continuous x-ray background, but the RHEED pattern did not show any remarkable change except for a slight decrease in intensity.[11] On the other hand, the subsequent Se exposure drastically increased the Se $K\alpha$ peak intensity, resulting in a change in the surface reconstruction from (2×4) to (2×1) characteristic of the Se-terminated GaAs(001) surface.[12] This means that the preceding Zn exposure has little effect to suppress Se adsorption on the GaAs(001)-(2×4) surface, which is consistent with the previous XPS results that the Zn coverage on the Zn-exposed (2×4) surface is much less than 1 monolayer (ML) in coverage.[13,14]

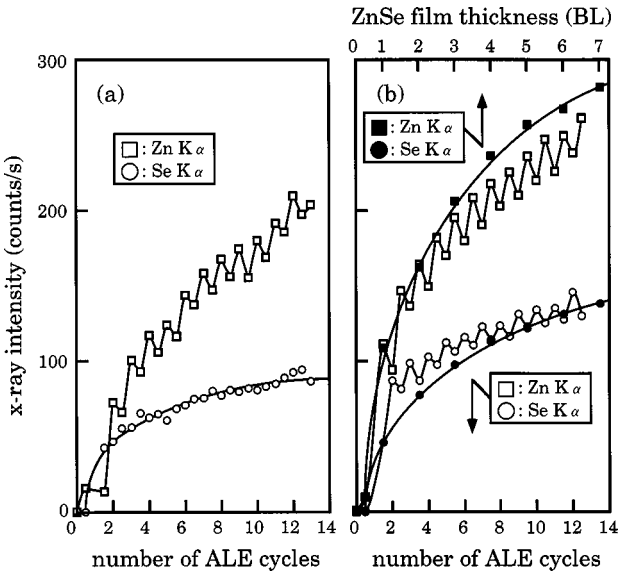

FIG. 1. Variations in the intensities of the Zn $K\alpha$ and Se $K\alpha$ lines during ALE growth of ZnSe. (a) Island growth on GaAs(001). (b) Layer-by-layer growth on ZnSe(1 BL)/GaAs(001). Lines are guides for the eyes.

As growth proceeded (>2 ALE cycles), the RHEED pattern changed from streaks to diffuse spots, indicating that ZnSe grows in an island mode. Numerous studies have shown that ZnSe grows in the layer-by-layer mode on the Zn-treated GaAs(001) surface and the island mode on the Se-terminated GaAs(001) surface.[10,15] Thus, the observed island growth can be ascribed to the formation of the Se-terminated GaAs(001) surface during the first Se exposure, as mentioned above.

In order to suppress such an unintentional reaction between Se and GaAs at the very initial stage of ALE growth, the Zn-treated GaAs(001) surface was exposed to both Zn and Se beams simultaneously for a predetermined period, typically 18 s. This procedure formed 1 BL of ZnSe, as confirmed by RHEED intensity oscillations for the MBE growth of ZnSe(001). Our RHEED observations have shown that the subsequent ALE growth proceeds in the layer-by-layer mode. Thus, for the RHEED rocking-curve analysis described in Sec. III B, the ZnSe(001) surface was prepared by ALE growth on ZnSe(1 BL)/GaAs(001).

Figure 1(b) shows the intensities of the Zn $K\alpha$ and Se $K\alpha$ lines emitted from the ZnSe(001) film growing in the layer-by-layer mode (open symbols). As can be seen in Figs. 1(a) and 1(b), below ~3 ALE cycles, both Zn $K\alpha$ and Se $K\alpha$ x-ray intensities for the layer-by-layer mode manifest themselves in higher rises than those for the island mode. Here, it should be noted that characteristic x-ray lines from rough surfaces have peaks at take-off angles lower than those for flat surfaces.[16] Thus, in order to compare x-ray peak intensi-

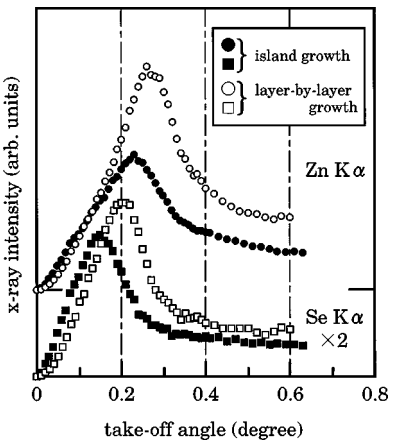

FIG. 2. Intensities of the Zn $K\alpha$ and Se $K\alpha$ lines from ZnSe(001) films plotted as a function of a take-off angle of the x-rays. For the measurements, growth was interrupted after 10 ALE cycles.

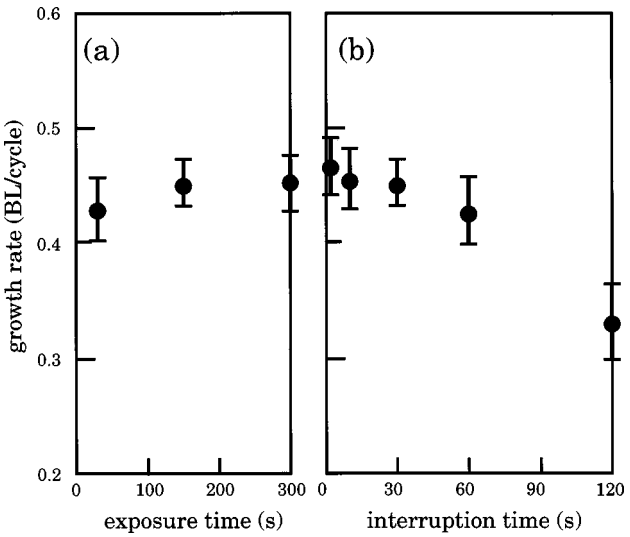

FIG. 3. The growth rate of ALE-grown ZnSe(001) films estimated by XPS measurements as a function of (a) the exposure time and (b) the growth interruption time.

ties for the layer-by-layer and island growth modes, it is necessary to measure these lines as a function of θ_t. The results are shown in Fig. 2. As we have expected, both lines for island growth have their peaks at angles lower than those for layer-by-layer growth. On the other hand, peak intensities for island growth are indeed lower than those for layer-by-layer growth. From these results, one may attribute the difference in x-ray intensity profiles [Figs. 1(a) and 1(b)] to the different growth modes, similarly to the case for Auger-electron spectroscopy analysis. However, in TRAXS measurements, it has been reported that x-ray intensities of a growing film at the very initial stage of growth (e.g., a few ML in thickness) are almost proportional to the amount of atoms deposited on a substrate surface, regardless of the growth mode.[17,18] Thus, the results in Figs. 1(a) and 1(b) lead us to conclude that the amount of deposited ZnSe (i.e., the growth rate) for island growth is smaller (lower) than that for layer-by-layer growth.

Another noteworthy finding in Fig. 1(b) is the intensity oscillation of x-rays: the Zn $K\alpha$ (Se $K\alpha$) intensity increases during Zn (Se) exposure. This means that the TRAXS has sensitivity high enough to study surface chemical composition of growing thin films.

From the results shown in Fig. 1(b), the growth rate of ZnSe can be estimated. For this purpose, we performed TRAXS measurements for ZnSe grown by MBE and compared the results with those for ALE growth. The MBE growth of ZnSe was carried out in an intermittent manner. The Zn shutter was first opened, and growth was initiated by opening the Se shutter for 18 s, which results in the formation of 1 BL of ZnSe. Each sequence was followed by *in situ* TRAXS measurements under the Zn beam. We have already reported that the ZnSe growth in the intermittent mode proceeds in the layer-by-layer mode.[15] The results are also plotted in Fig. 1(b) (closed symbols) as a function of film thickness. If we assume that 1 BL thickness corresponds to 2–2.5 ALE cycles, a good agreement between x-ray intensities for MBE growth and ALE growth is obtained. This indicates that ALE growth proceeds at a rate of 0.4–0.5 BL/cycle.

The growth rate of 0.4–0.5 BL/cycle was also confirmed by XPS measurements that were carried out by using monochromatic Al $K\alpha$ radiation (1486.6 eV). For XPS measurements, growth was interrupted after 10 ALE cycles and the thickness of ZnSe was evaluated from the photoelectron-peak intensities. The substrate intensity I_S attenuates as $I_S/I_{S0}=\exp(-d/\lambda \sin\theta)$ with film thickness d, while the overlayer intensity I_C increases as $I_C/I_{C0}=1-\exp(-d/\lambda \sin\theta)$, where I_{S0} and I_{C0} are the intensities for semi-infinite GaAs and ZnSe, respectively. The constant λ is the mean-free path of the photoelectrons, which is assumed to be the same for both the substrate and overlayers ($\lambda=16$ Å).[19] θ is the emission angle, which is 35° in our setup. We have confirmed that the thickness of MBE-grown ZnSe(001) films, which is estimated by using above equations, agrees well with that determined by RHEED intensity oscillations.[20] Figure 3(a) shows growth rates of ZnSe as a function of the exposure time. As can be seen in Fig. 3(a), the growth rate for exposure time longer than 150 s is estimated to be ~0.45 BL/cycle, which is in good agreement with the TRAXS results.

These results are consistent with RHEED observations. Figures 4(a)–4(d) show changes in specular-beam intensity measured along the [110] direction during ALE growth. Changes in the intensities with a period of 2 ALE cycles are clearly seen, especially for glancing angles of 0.8 and 1.8°. Thus, TRAXS, XPS, and RHEED results all indicate that the ALE growth proceeds at a rate of ~0.5 BL/cycle.

Another interesting finding in Fig. 4 is that the growing ZnSe surface under the Zn beam has a higher specular-beam intensity than the surface under the Se beam for electron-beam incidence at 0.8, 1.8, and 2.5°, while the result at 1.2° is opposite. Such behaviors in RHEED intensities is likely to be related to the reconstructed structures of the ZnSe(001) surfaces, which will be discussed later in this paper.

B. Surface structures of ZnSe(001)

As mentioned in the Introduction, since the ALE growth of ZnSe(001) proceeds forming two alternating reconstructions of (2×1) and $c(2\times2)$, the growth mechanism is

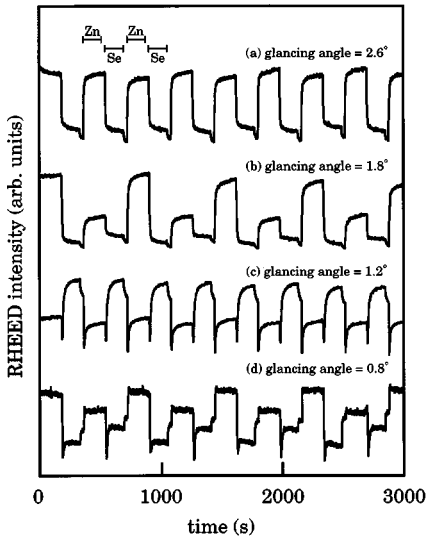

FIG. 4. Changes in the specular-beam intensity during ALE growth of ZnSe measured at glancing angles of (a) 2.5°, (b) 1.8°, (c) 1.2°, and (d) 0.8°.

strongly related with the atomic structures of these reconstructed surfaces. Previous studies based on first-principles total-energy calculations have shown that the Se-stabilized ZnSe(001)-(2×1) and Zn-stabilized ZnSe(001)-$c(2\times2)$ surfaces have the Se-dimer [Fig. 5(a)] and Zn-vacancy structures [Fig. 5(b)], respectively.[22,23] The former has a

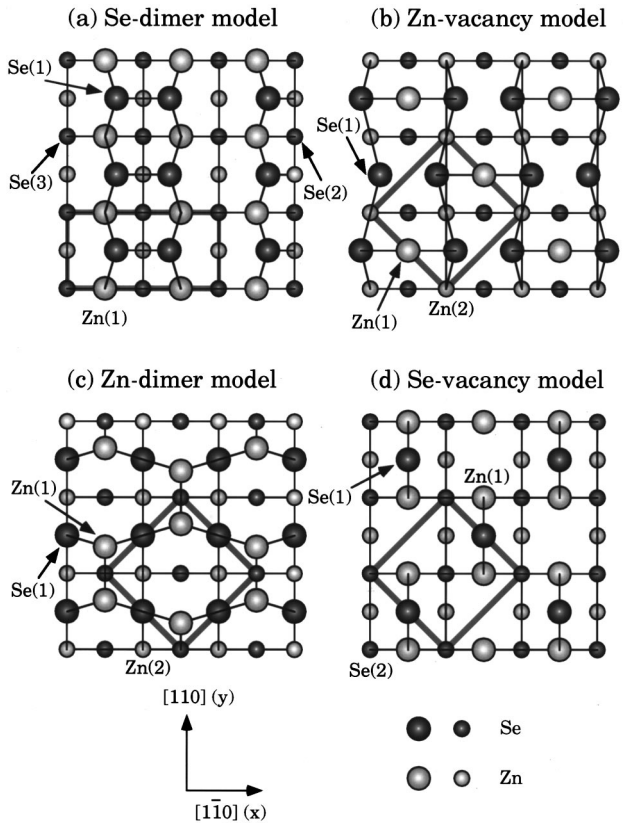

FIG. 5. Top views of surface reconstruction models for the ZnSe(001)-(2×1) (a) and $-c(2\times2)$ surfaces (b)–(d). (a) Se-dimer model; (b) Zn-vacancy model; (c) Zn-dimer model; (d) Se-vacancy model.

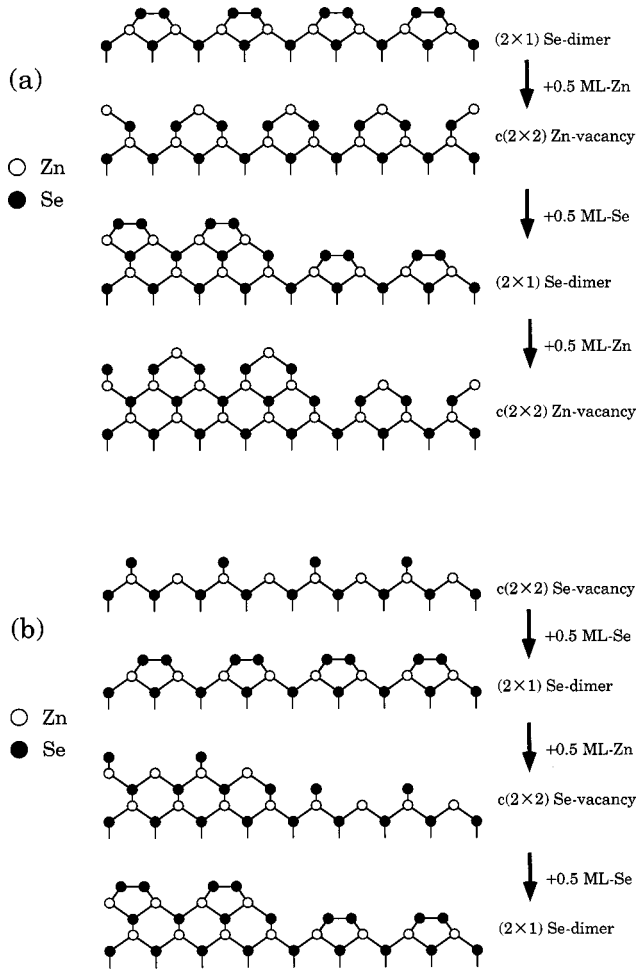

FIG. 6. Schematic views in the (110) plane of ZnSe(001) showing the surface features during ALE growth of ZnSe(001). (a) The alternate formation of the (2×1) Se-dimer and the $c(2\times2)$ Zn-vacancy structures. (b) The alternate formation of the (2×1) Se-dimer and the $c(2\times2)$ Se-vacancy structures.

surface-Se coverage of 1.0 ML, while the latter has a surface-Zn coverage of 0.5 ML. Thus, as shown in Fig. 6(a), the alternate formation of these reconstructions results in the growth rate of 0.5 BL/cycle,[24] in good agreement with the results shown in the preceding subsection. Although these structure models have also been confirmed by photoemission spectroscopy experiments,[25–27] there is practically no experimental information about their atomic coordinates.

In order to study the atomic structures of ZnSe(001) and to correlate them with the changes in RHEED intensities shown in Fig. 4, we performed RHEED rocking-curve analysis on the basis of the dynamical diffraction theory.[28] Integrated intensities of RHEED for the (2×1) and $c(2\times2)$ surfaces were calculated by the multislice method[28] using 13 beams and 7 beams on the zeroth Laue zone with the incident electron beam along the [110] direction, respectively: (0 0), $(\pm\frac{1}{2}\ 0)$, $(\pm1\ 0)$, $(\pm\frac{3}{2}\ 0)$, $(\pm2\ 0)$, $(\pm\frac{5}{2}\ 0)$, and $(\pm3\ 0)$ for (2×1), and (0 0), $(\pm1\ 0)$, $(\pm2\ 0)$, and $(\pm3\ 0)$ for $c(2\times2)$. The Fourier components of the crystal potential for elastic scattering was derived from the electron scattering factors for Zn and Se tabulated by Doyle and Tuner.[29] We include a correction to the Fourier component of the potential so that the mean inner potential is consistent with the

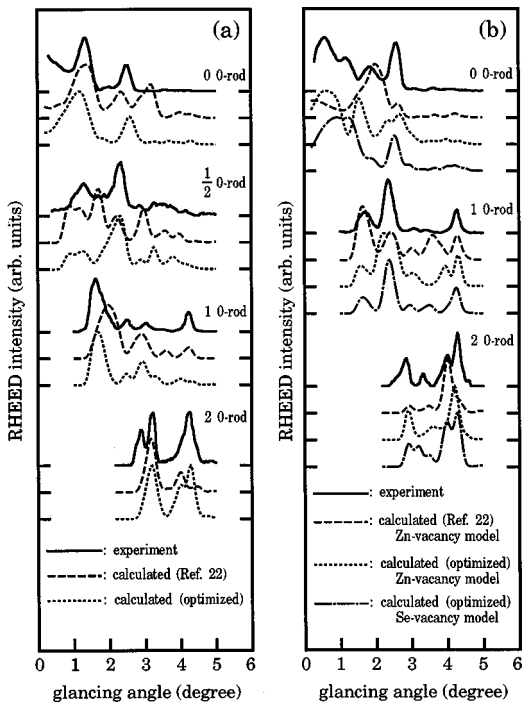

FIG. 7. RHEED rocking curves (solid curves) measured from the ZnSe(001)-(2×1) (a) and ZnSe(001)-c(2×2) (b) surfaces. The dashed, dotted, and dashed-dotted curves are calculated from the atomic coordinates listed in Table I.

value estimated from the present experiment, i.e., −12.3 eV. The adsorption of electrons in a crystal is given phenomenologically by an imaginary potential. The imaginary potential for bulk ZnSe is assumed to be 10% of its real part, while that for atoms in the first and second bilayer was treated as a fitting parameter. The thickness of a slice, in which scattering potential was approximated to be constant toward the surface normal direction, was about 0.1 Å. In order to quantify the agreement between the calculated rocking curves and the experimental ones, the R factor defined as

$$R=\frac{1}{N}\sum_{g}\frac{\int[I_{go}(\theta)-c_g I_{gc}(\theta)]^2 d\theta}{\int[I_{go}(\theta)]^2 d\theta},\quad c_g=\frac{\int I_{go}(\theta)d\theta}{\int I_{gc}(\theta)d\theta},$$

was used.[30] Here, I_{go} and I_{gc} are the observed and the calculated intensities of beam g as a function of glancing angle θ, respectively, and N is the number of analyzed beams. The calculated rocking curves were convoluted with a Gaussian, which has a full width at half maximum of 0.1°, corresponding to the experimental resolution.

Figure 7 shows RHEED rocking curves (solid curves) measured from the ZnSe(001)-(2×1) and ZnSe(001)-c(2×2) surfaces, together with the calculated ones (dashed curves) from the structure models proposed by Park and Chadi.[22] The Se-dimer and the Zn-vacancy models gave large R factors of 0.508 and 0.635, respectively, suggesting that the present results are incompatible with the atomic coordinates given in Ref. 22. In order to obtain better agreement between the measured and calculated rocking curves, the atomic coordinates were optimized. Since the present analysis has been carried out using the beams on the zeroth Laue zone at [110] incidence, only information about the structure projected on the (110) plane is available. Thus, the atomic coordinates along the [110] direction were excluded from being structural parameters. The atomic coordinates were optimized as follows. Firstly, the atomic coordinates of the first-layer atoms were changed holding others identical to those given in Ref. 22, so as to minimize the R factor. Secondly, starting from the optimized structure at this stage, the atomic coordinates of the second- and third-layer atoms were refined one after another. Finally, the resulting optimized structure was set as the starting point of the next refinement. This procedure iteratively minimizes the R factor. The minimum in the R factor was typically reached after 10 steps of iteration.

TABLE I. Atomic displacement from bulk positions for the optimized surface structures for ZnSe(001) (in Å). The x and z displacements are along the [110] and [001] directions, respectively.

Notation in Fig. 4	Park and Chadi (Ref. 22)		This study	
	x	z	x	z
		(2×1) Se-dimer		
Se (1)	+0.76	+0.03	+0.45±0.07	+0.09±0.13
Zn (1)	+0.22	+0.04	+0.16±0.08	−0.30±0.06
Se (2)	0.00	−0.15	0.00	−0.58±0.16
Se (3)	0.00	+0.26	0.00	−0.35±0.07
		c(2×2) Zn-vacancy		
Zn (1)	0.00	−1.28	0.00	−0.93±0.09
Se (1)	+0.23	+0.02	+0.50±0.08	−0.47±0.21
Zn (2)	0.00	−0.01	0.00	−0.28±0.09
		c(2×2) Zn-dimer		
Zn (1)			0.00	+0.79±0.15
Se (1)			0.00	+0.12±0.12
Zn (2)			0.00	+0.12±0.19
		c(2×2) Se-vacancy		
Se (1)	0.00	+0.06	0.00	+0.30±0.07
Zn (1)	0.00	−0.18	0.00	+0.12±0.07
Se (2)	0.00	−0.08	0.00	+0.18±0.05

Shown by dotted curves in Figs. 7(a) and 7(b) are rocking curves calculated from the optimized Se-dimer and Zn-vacancy models for which the atomic displacements from bulk positions are listed in Table I. Errors of the atomic coordinates in Table I were evaluated from the half width of the range where the R factor is smaller than $1.1\times R_{\min}$.[30] On one hand, the agreement is considerably improved for Se-stabilized (2×1) ($R_{\min}=0.159$). On the other hand, Zn-stabilized c(2×2) still gave a relatively large R factor of 0.216. In particular, peaks at 1.2 and 1.8° in the measured rocking curve of the (0 0) beam are not reproduced in the calculated rocking curve. This result prompted us to test some other possible structure models for the c(2×2) surface. The rocking curves calculated from the Zn-dimer model [Fig. 5(c)] disagree with the experimental curves ($R_{\min}=0.276$), while for the Se-vacancy model [Fig. 5(d)], the most of features in the measured rocking curves are well reproduced in the calculated rocking curves (dashed-dotted curves in Fig. 7). The R factor of the Se-vacancy model is 0.128 showing a good agreement between the experiment and the calculation.

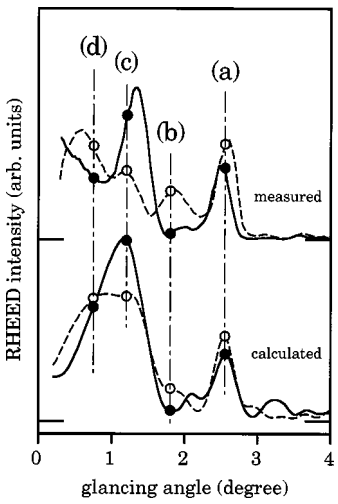

FIG. 8. Comparison of RHEED rocking curves for ZnSe(001)-(2×1) (solid curves) and the ZnSe(001)-$c(2\times2)$ (dashed curves). The points (a)–(d) correspond to the glancing angles at which the changes in the specular beam intensity were monitored during ALE growth (Fig. 4).

In Fig. 8, we compare rocking curves for the (2×1) Se-dimer and $c(2\times2)$ Se-vacancy structures. For both measured and calculated rocking curves, the $c(2\times2)$ surface has a higher specular-beam intensities (open circles) than those for the (2×1) (closed circles), except for the case at 1.2°. This is in accord with changes in RHEED intensities shown in Fig. 4. On the other hand, rocking curves calculated for the Zn-vacancy model [Fig. 5(b)] are incompatible with the results in Fig. 4. Thus, the results in Figs. 4 and 8 further support the present analysis that the (2×1) and $c(2\times2)$ surfaces have the Se-dimer and Se-vacancy structures, respectively.

As mentioned at the opening paragraph of this subsection, theoretical calculations[22,23] and photoemission spectroscopy experiments[25–27] have shown that the $c(2\times2)$ surface has the Zn-vacancy structure. This stands in clear contrast to the present analysis. Although the reason for such a disagreement with the theoretical results[22,23] still remains unclear, the Se-vacancy model can be consistent with the experimental data in Refs. 25–27, on the basis of the following reasons. Similarly to the case for the Zn-vacancy model, the Se-vacancy model has equal numbers of Zn and Se dangling bonds [two of each kind per $c(2\times2)$ unit cell]. According to the electron counting model,[31] transfer of 1/2 electron from each Zn dangling bond to each Se-dangling bond transforms the Se- and Zn- dangling bonds into fully occupied and empty states, respectively, so that the $c(2\times2)$ surface is electronically stabilized, not leaving any partially filled dangling bonds. Thus, the Se-vacancy model can explain the photoemission spectroscopy results for the $c(2\times2)$ surface;[25–27] (i) core-level spectra for Zn and Se have similar intensity ratios of the surface to bulk components, and (ii) the surface Zn and Se components are shifted toward higher and lower binding energies, respectively, with respect to their bulk components.

In Fig. 6(b), we propose a possible ALE mechanism that explain the switching between the (2×1) Se-dimer and $c(2\times2)$ Se-vacancy surfaces. Similarly to the case in Fig. 6(a), growth rate of 0.5 BL/cycle is expected. However, the reason why the growth rate estimated by TRAXS and XPS ($\sim$0.45 BL/cycle) is slightly less than 0.5 BL/cycle still remains unexplained. This can be explained by considering the desorption of Zn or Se from growing ZnSe surfaces during growth interruption. In order to confirm this, we performed ALE growth experiments changing the time of growth interruption. Figure 3(b) shows the growth rate estimated by XPS measurements, in which the growth rate indeed decreases as the interruption time is increased. Since the desorption of Zn from the $c(2\times2)$ surface hardly occurs at temperatures below 400 °C even under the irradiation of electron beam,[32] it appears likely that the decrease in the growth rate is due to the desorption of Se. The Se desorption during the growth interruption is also evidenced by RHEED observations. As can be seen in Fig. 4, RHEED intensities changed immediately after the Se beam was turned off, while no change was observed after the Zn shutter was closed. Here, we note that in the present experiment the effects of the electron-beam irradiation on the Se desorption [32] is negligible, because ALE growth experiments with and without RHEED observations gave the same growth rates.

IV. CONCLUSIONS

We have studied the structure and composition of the ZnSe(001) surface during ALE growth using RHEED and TRAXS in real time. The ZnSe(001) surface has the (2×1) Se-dimer and $c(2\times2)$ Se-vacancy structures under the Se and Zn beams, respectively. Contrary to the previously proposed Zn-vacancy model, the latter is not terminated with a half monolayer of Zn atoms, but, with a half monolayer of Se atoms. The ALE growth proceeds at a rate of 0.5 BL per ALE cycle, which is expected from the alternate formation of the (2×1) Se-dimer and $c(2\times2)$ Se-vacancy structures.

ACKNOWLEDGMENTS

This study, partly supported by the New Energy and Industrial Technology Development Organization, was performed at the Joint Research Center for Atom Technology under the research agreement between the National Institute for Advanced Interdisciplinary Research and the Angstrom Technology Partnership. We would like to acknowledge encouragement from K. Kimura, S. Miwa, L. H. Kuo, C. G. Jin, and M. Ozeki.

[1] T. Yao and T. Takeda, Appl. Phys. Lett. **48**, 160 (1986).

[2] Z. Zhu, M. Hagino, K. Uesugi, S. Kamiyama, M. Fujimoto, and T. Yao, J. Cryst. Growth **99**, 441 (1990); Jpn. J. Appl. Phys., Part 1 **28**, 1659 (1989).

[3] One bilayer is defined as one atomic layer of Zn plus one atomic layer of Se.

[4] S. Dosho, Y. Takemura, M. Konagai, and K. Takahashi, J. Appl. Phys. **66**, 2597 (1989).

[5] S. Bauer, H. Berger, P. Link, and W. Gebhardt, J. Appl. Phys. **74**, 3916 (1993).
[6] J. M. Gaines and C. A. Ponzoni, Surf. Sci. **290**, 172 (1993).
[7] S. Hasegawa, S. Ino, Y. Yamamoto, and H. Daimon, Jpn. J. Appl. Phys., Part 2 **24**, L387 (1985).
[8] T. Yasuda, L. H. Kuo, K. Kimura, S. Miwa, C. G. Jin, K. Tanaka, and T. Yao, J. Vac. Sci. Technol. B **14**, 3052 (1996).
[9] L. H. Kuo, K. Kimura, T. Yasuda, S. Miwa, C. G. Jin, K. Tanaka, and T. Yao, Appl. Phys. Lett. **68**, 2413 (1996).
[10] A. Ohtake, S. Miwa, L. H. Kuo, T. Yasuda, K. Kimura, C. G. Jin, and T. Yao, J. Cryst. Growth **184/185**, 163 (1998).
[11] S. Miwa, L. H. Kuo, K. Kimura, T. Yasuda, and T. Yao, Jpn. J. Appl. Phys., Part 2 **36**, L337 (1997).
[12] M. D. Pashley and D. Li, J. Vac. Sci. Technol. A **12**, 1848 (1994).
[13] S. Miwa, L. H. Kuo, K. Kimura, T. Yasuda, A. Ohtake, C. G. Jin, and T. Yao, Appl. Phys. Lett. **73**, 939 (1998).
[14] S. Heun, J. J. Paggel, S. Rubini, and A. Franciosi, J. Vac. Sci. Technol. B **14**, 2980 (1996).
[15] T. Yasuda, K. Kimura, S. Miwa, L. H. Kuo, A. Ohtake, C. G. Jin, K. Tanaka, and T. Yao, J. Vac. Sci. Technol. B **15**, 1212 (1997).
[16] S. Shimizu, K. Yamamuro, K. Fuwa, H. Yanagida, H. Yamakawa, and S. Ino, Thin Solid Films **228**, 18 (1993).
[17] S. Hasegawa, H. Daimon, and S. Ino, Surf. Sci. **186**, 138 (1987).
[18] We note that slight and gradual changes in the gradient for all curves beyond ~3 ALE cycles are not due to the decrease in the growth rate, but are ascribed to the self-adsorption effect of x-rays.
[19] A. Ohtake, S. Miwa, L. H. Kuo, K. Kimura, T. Yasuda, C. G. Jin, and T. Yao, Phys. Rev. B **56**, 14 909 (1997).
[20] We note that the film thickness of ZnSe on GaAs(001) determined by RHEED intensity oscillations agrees well with those measured using high-resolution Rutherford backscattering spectroscopy (Ref. 21) and high-resolution cross-sectional transmission electron microscopy (Ref. 15).
[21] A. Ohtake, L. H. Kuo, K. Kimura, S. Miwa, T. Yasuda, C. G. Jin, T. Yao, K. Nakajima, and K. Kimura, Phys. Rev. B **57**, 1410 (1998).
[22] C. H. Park and D. J. Chadi, Phys. Rev. B **49**, 16 467 (1994).
[23] A. García and J. E. Northrup, Appl. Phys. Lett. **65**, 708 (1994).
[24] Similar growth model has been proposed for ALE growth of ZnTe(001). [B. Daudin, S. Tatarenko, and D. Brun-Le Cunff, Phys. Rev. B **52**, 7822 (1995)].
[25] W. Chen, A. Kahn, P. Soukiassian, P. S. Mangat, J. Gaines, C. Ponzoni, and D. Olego, J. Vac. Sci. Technol. B **12**, 2639 (1994).
[26] W. Chen, A. Kahn, P. Soukiassian, P. S. Mangat, J. Gaines, C. Ponzoni, and D. Olego, Phys. Rev. B **49**, 10 790 (1994).
[27] H. H. Farrell, M. C. Tamargo, S. M. Shibli, and Y. Chang, J. Vac. Sci. Technol. B **8**, 884 (1990).
[28] A. Ichimiya, Jpn. J. Appl. Phys., Part 1 **22**, 176 (1983) **24**, 1365 (1985).
[29] P. A. Doyle and P. S. Turner, Acta Crystallogr., Sect. A: Cryst. Phys., Diffr., Theor. Gen. Crystallogr. **A24**, 390 (1968).
[30] T. Hanada, S. Ino, and H. Daimon, Surf. Sci. **313**, 143 (1994); T. Hanada, H. Daimon, and S. Ino, Phys. Rev. B **51**, 13 320 (1995).
[31] M. D. Pashley, Phys. Rev. B **40**, 10 481 (1989).
[32] M. Ohishi, H. Saito, H. Torihara, Y. Fujisaki, and K. Ohmori, Jpn. J. Appl. Phys., Part 1 **30**, 1647 (1991).